

Article

Combined Effects of Meteorological Factors, Terrain, and Greenhouse Gases on Vegetation Phenology in Arid Areas of Central Asia from 1982 to 2021

Ruikang Tian ¹, Liang Liu ¹, Jianghua Zheng ^{1,2,*}, Jianhao Li ¹, Wanqiang Han ¹ and Yujia Liu ¹¹ College of Geography and Remote Sensing Science, Xinjiang University, Urumqi 830046, China² Xinjiang Key Laboratory of Oasis Ecology, Xinjiang University, Urumqi 830046, China

* Correspondence: zheng.jianghua@xju.edu.cn

Abstract: Spatiotemporal variations in Central Asian vegetation phenology provide insights into arid ecosystem behavior and its response to environmental cues. Nevertheless, comprehensive research on the integrated impact of meteorological factors (temperature, precipitation, soil moisture, saturation vapor pressure deficit), topography (slope, aspect, elevation), and greenhouse gases (carbon dioxide, methane, nitrous oxide) on the phenology of Central Asian vegetation remains insufficient. Utilizing methods such as partial correlation and structural equation modeling, this study delves into the direct and indirect influences of climate, topography, and greenhouse gases on the phenology of vegetation. The results reveal that the start of the season decreased by 0.239 days annually, the length of the season increased by 0.044 days annually, and the end of the season decreased by 0.125 days annually from 1982 to 2021 in the arid regions of Central Asia. Compared with topography and greenhouse gases, meteorological factors are the dominant environmental factors affecting interannual phenological changes. Temperature and vapor pressure deficits (VPD) have become the principal meteorological elements influencing interannual dynamic changes in vegetation phenology. Elevation and slope primarily regulate phenological variation by influencing the VPD and soil moisture, whereas aspect mainly affects the spatiotemporal patterns of vegetation phenology by influencing precipitation and temperature. The findings of this study contribute to a deeper understanding of how various environmental factors collectively influence the phenology of vegetation, thereby fostering a more profound exploration of the intricate response relationships of terrestrial ecosystems to environmental changes.

Keywords: structural equation modeling; climate; topography; vapor pressure deficit; vegetation phenology



Citation: Tian, R.; Liu, L.; Zheng, J.; Li, J.; Han, W.; Liu, Y. Combined Effects of Meteorological Factors, Terrain, and Greenhouse Gases on Vegetation Phenology in Arid Areas of Central Asia from 1982 to 2021. *Land* **2024**, *13*, 180. <https://doi.org/10.3390/land13020180>

Academic Editor: Iva Apostolova

Received: 3 January 2024

Revised: 24 January 2024

Accepted: 30 January 2024

Published: 3 February 2024



Copyright: © 2024 by the authors. Licensee MDPI, Basel, Switzerland. This article is an open access article distributed under the terms and conditions of the Creative Commons Attribution (CC BY) license (<https://creativecommons.org/licenses/by/4.0/>).

1. Introduction

Vegetation plays a crucial role in the exchange of energy, water, and carbon between the Earth's surface and atmosphere, making it a fundamental component of terrestrial ecosystems [1,2]. Vegetation phenology refers to phenomena in the life cycle of plants related to seasonal changes. Vegetation phenology plays a critical role in global ecosystems because it reflects how ecosystems respond to climate and environmental changes [3,4]. As global climate change intensifies and greenhouse gas emissions increase, vegetation phenology has gradually become a focal point of research in multiple fields, including ecology, meteorology, and environmental science [3,5,6]. Therefore, understanding how vegetation phenology responds to various environmental factors is beneficial for effective land ecosystem management and provides valuable insights with respect to the adaptation of humans to environmental changes.

Changes in vegetation phenology are vital for ecosystem stability, productivity, and the provision of ecological services [7,8]. The results of previous research indicated that

vegetation phenology is influenced by various environmental factors, including meteorological factors, topography, and greenhouse gas emissions [9–11]. In previous studies, the effects of climatic factors on vegetation phenology were elucidated. Piao et al. (2007) reported that rising temperatures significantly advance the spring phenology in the high- and mid-latitude regions of the Northern Hemisphere [12]. Luo et al. (2021a) discovered that an increase in spring soil moisture (SM) leads to an earlier start of the season (SOS) on the Mongolian Plateau, whereas increased summer SM causes a delay at the end of the season (EOS) [13]. Topography and landscape play critical roles in shaping the patterns of phenological changes. Yang et al. (2020) stated that this aspect plays a key role in influencing vegetation patterns in semiarid regions [14]. Chen et al. (2020) discovered that elevation influences the correlation between Chinese vegetation and abnormal precipitation [15]. Greenhouse gases also significantly affect vegetation phenology. Among others, Norby and Zak (2011) reported that elevated CO₂ concentrations promote vegetation growth [16]. In a study on the drivers of global vegetation growth, Liu et al. (2023) observed a positive sensitivity of the NDVI to the atmospheric CO₂ concentration [17]. Nevertheless, previous research has typically focused on the impact of singular categories of environmental factors on vegetation dynamics, overlooking the direct and indirect influences of diverse environmental factors on phenology. The integrated impact of meteorological factors, greenhouse gases, and topography on vegetation phenology remains unclear.

Central Asia occupies a central position on the Eurasian continent, connecting Europe, Asia, and the Middle East. It plays a pivotal role in geopolitical affairs, regional security, and cultural exchanges [18]. In recent years, the climate in Central Asia has undergone significant changes, including temperature increases exceeding global land averages, regional disparities, seasonal variations in precipitation distribution, and rising emissions of greenhouse gases, exacerbating climate change uncertainties [19–21]. The complex terrain of Central Asia, along with its unique climate and ecosystems, makes its response to global climate change intricate and sensitive [22]. Wu et al. (2021a) reported that meteorological factors led to a delay in the vegetation SOS and advancement in the EOS in Central Asia from 2000 to 2019 [23]. Among others, Gao and Zhao (2022) stated that meteorological factors resulted in a significant advancement of both SOS and EOS in Central Asia from 1982 to 2014, with changes of -0.143 days per year and -0.363 days per year, respectively [24]. These researchers primarily focused on the effects of meteorological factors on the phenology of Central Asian vegetation. The combined effects of meteorological factors, greenhouse gases, and topography on the phenology of Central Asian vegetation remain unknown.

To better comprehend how vegetation in the arid regions of Central Asia responds and adapts to environmental changes, it is imperative to delineate the direct and indirect influences of climate, topography, and greenhouse gases on vegetation phenology. This study utilized NOAA CDR NDVI products spanning from 1982 to 2021 to extract vegetation phenological indicators (SOS, EOS, and LOS) and distribution information. The investigation delves into the geographical evolution of vegetation phenology and explores the relationships between phenological indicators and environmental variables. The objectives of this study include: (1) analyzing the impact of meteorological factors on vegetation phenology; (2) examining the relationship between topography and vegetation phenology; (3) investigating the direct and indirect influences of meteorological factors, topography, and greenhouse gases on Central Asian vegetation phenology. The outcomes of this study contribute to a profound understanding of the response mechanisms of terrestrial ecosystems to complex environmental changes, providing scientific foundations for sustainable development and environmental conservation.

2. Materials and Methods

2.1. Study Area

Central Asia is situated deep within the Eurasian landmass, far from the oceans, isolating its geographical location (Figure 1a). The climate in this region predominantly manifests

as a classic temperate continental climate with vast expanses of deserts and steppes. Because of its inland position and the absence of maritime influence, compounded by the effect of high mountainous terrain to the southeast, Central Asia experiences enduringly scanty precipitation, marked by a distinctively uneven distribution [25]. Summer temperatures soar, whereas winters bring frigid conditions. The annual average precipitation generally remains below 300 mm, with some areas receiving less than 200 mm, resulting in severe aridity [26]. Central Asia encompasses a diverse landscape comprising hills, plains, lowlands, and mountainous terrain. Its vegetation array is rich and varied, primarily dominated by grasslands but also includes shrublands, forests, and cultivated fields (Figure 1b). The effect of greenhouse gas emissions on the climate has gradually intensified in Central Asia. These geographical, climatic, topographical, and vegetative characteristics collectively constitute the unique natural environment of Central Asia, rendering it a pivotal subject of study in the realms of geography and climate research.

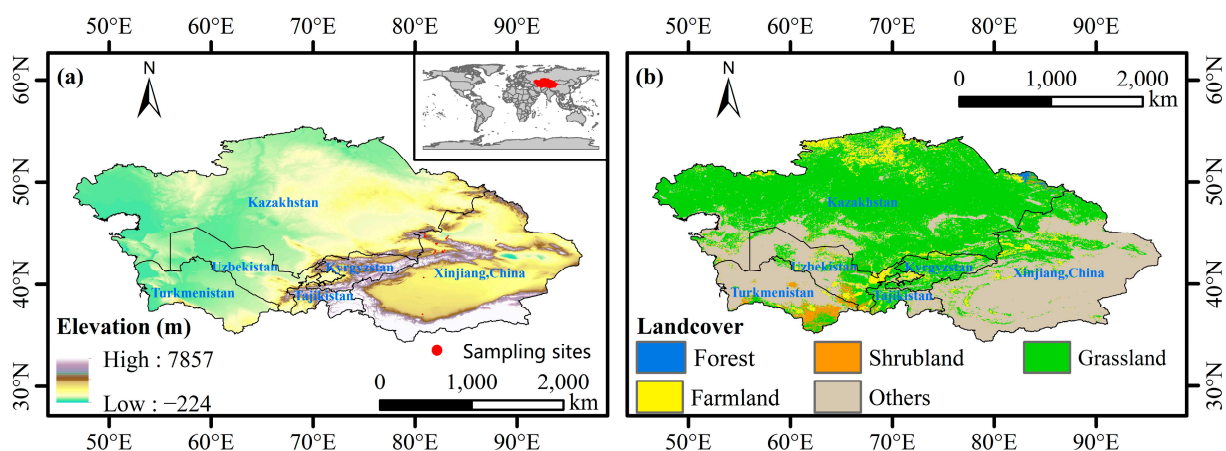


Figure 1. (a) Elevation data and (b) Distribution of vegetation types in Central Asia.

2.2. Data

2.2.1. NDVI and Phenological Validation Data

NOAA CDR NDVI data, spanning 1982–2021, feature a spatial resolution of 0.05° and a temporal resolution of one day (Normalized Difference Vegetation Index CDR | National Centers for Environmental Information (NCEI) (noaa.gov) (accessed on 1 January 2023)). Phenological field data are sourced from the primary ecological observation stations in China (CERN) (<http://www.cern.ac.cn/0index/index.asp> (accessed on 1 January 2023)) and the greening period monitoring data of $1\text{ m} \times 1\text{ m}$ plots in Xinjiang from 2018 to 2021. This includes phenological observations from stations in Fukang, Cele, Yili, and Aksu, documenting budburst, flowering, fruiting, and seed dispersal periods. The budburst period is defined as 50% vegetation regreening within the sample plot, hence we selected the budburst period as the observed validation data for Start of Season (SOS).

2.2.2. Climate Data

Land surface temperature, dew point temperature, precipitation, and multilevel SM data from 1982 to 2021 were sourced from the ERA5 dataset provided by the European Center for Medium-Range Weather Forecasts (ECMWF). These data have a spatial resolution of 0.1° and a monthly temporal resolution. Notably, SM data represent the average values across three depth layers, that is, 0–7, 7–28, and 28–100 cm, collectively reflecting the SM conditions within the root zone.

The calculation of the vapor pressure deficit (VPD) in the atmosphere is based on the land surface and dew point temperatures:

$$Q_a = Q_b \left(\frac{T_m + 273.16}{T_m + 273.16 + 0.0065 \times D} \right)^{5.625} \quad (1)$$

$$C_d = 1 + 7 \times 10^{-4} + 3.46 \times 10^{-6} Q_a \quad (2)$$

$$SVP = 6.112 \times C_d \times e^{\frac{17.67T_m}{T_m+243.5}} \quad (3)$$

$$AVP = 6.112 \times C_d \times e^{\frac{17.67T_n}{T_n+243.5}} \quad (4)$$

$$VPD = SVP - AVP, \quad (5)$$

where T_m is the land surface temperature ($^{\circ}\text{C}$), T_n is the dew point temperature ($^{\circ}\text{C}$), D is the elevation above sea level (m), Q_a is the air pressure (hPa), Q_b is the mean sea-level pressure (1013.25 hPa), SVP is the saturation vapor pressure, and AVP is the actual vapor pressure.

2.2.3. Topographical Data and Vegetation Types

Vegetation-type data for the arid region of Central Asia were derived from the 2000 version of the MCD12Q1 dataset with a spatial resolution of 500 m (accessible at <https://ladsweb.modaps.eosdis.nasa.gov/> (accessed on 1 January 2023)). Areas covered by waterbodies, barren land, unused land, cultivated land, forests, grasslands, and shrublands were excluded. Shuttle Radar Topography Mission Elevation data (SRTM DEM) with a spatial resolution of 30 m were sourced from NASA (available at <https://appears.earthdatacloud.nasa.gov/> (accessed on 1 January 2023)). ArcGIS 10.8 software was used to compute the surface slope and aspect. In this study, we included an elevation range from 0 to 4000 m at intervals of 100 m to discern the trends in vegetation phenology with changing elevation. Simultaneously, we investigated slope angles ranging from 0° to 50° and analyzed them at 1° intervals to determine the effect of the slope on vegetation phenology. The slope aspects were categorized into eight directions: North, Northeast, East, Southeast, South, Southwest, West, and Northwest, following the method employed by Bindajam et al. (2020) [27], with each direction spaced at 45° intervals. We examined the effects of different aspects on vegetation phenology by computing the mean vegetation phenological indicators in these eight directions.

2.2.4. Greenhouse Gas Data

Greenhouse gas emission data for carbon dioxide (CO_2), nitrous oxide (N_2O), and methane (CH_4) with a spatial resolution of 0.1° and an annual temporal resolution were obtained from the Emissions Database for Global Atmospheric Research (EDGAR; accessible at <https://edgar.jrc.ec.europa.eu/> (accessed on 1 January 2023)).

To ensure data consistency, we performed bilinear interpolation to resample Climate data, Topographical data and vegetation types, and Greenhouse gas data, adjusting the spatial resolution to 0.05° .

2.3. Methods

2.3.1. Extraction of Vegetation Phenology

The utilization of the Gaussian filtering method has significant importance and clear advantages for the extraction of vegetation phenology [28]. The Gaussian filtering technique, that is, the application of a Gaussian kernel function to temporally adjacent data points, allows weighted averaging, thereby aiding in the suppression of high-frequency noise in the data. This, in turn, enables the more precise capture of trends in phenological changes in the vegetation. Within the field of phenology extraction, three widely adopted methods are the dynamic threshold, piecewise logistic function, and modified double logistic function, each possessing distinct advantages and suitable scenarios:

- (1) **Dynamic Threshold Method:** This method relies on dynamic changes within time-series data and employs adaptive thresholds to determine the inflection points of phenological stages [29]. Its advantage lies in its capacity to automatically adjust

thresholds based on the data characteristics of different regions and years, rendering it highly versatile. The equation for the dynamic threshold method is as follows:

$$P = \frac{\text{NDVI}_t - \text{NDVI}_{\min}}{\text{NDVI}_{\max} - \text{NDVI}_{\min}}, \quad (6)$$

where daily NDVI values are represented by NDVI_t and NDVI_{\max} and NDVI_{\min} denote the maximum and minimum values of the NDVI curve during the observation period, respectively. The timings of the SOS and EOS are established as the dates when the ratio P rises to 0.2 and declines to 0.2, respectively [30].

- (2) Piecewise Logistic Function Method: Based on this method, a phenological curve is divided into multiple linear or nonlinear segments, and logistic functions are employed to describe the characteristics of each segment. This approach is sensitive to nuanced phenological changes and can capture intricate phenological patterns [31,32]. The typical equation for the piecewise logistic function method is as follows:

$$\text{NDVI}_i = \begin{cases} \frac{s_1}{1+e^{m_1+n_1k}} + r_1, & i \leq t \\ \frac{s_2}{1+e^{m_2+n_2k}} + r_2, & i > t' \end{cases} \quad (7)$$

where NDVI_i represents the NDVI value for the i -th day; t represents the date (day of year, DOY) when the NDVI reaches its maximum value; and m , n , s , and r denote the four key parameters of the rising and falling phase functions, respectively.

- (3) Modified Double Logistic Function Method: The modified double logistic function method improves upon the traditional double logistic function method to better suit the phenological extraction for various vegetation types. This method considers the effect of the vegetation type on phenology and has higher precision [33]. The modified double logistic function method employs two logistic functions, each dedicated to extracting growing and dormant seasons:

$$\text{NDVI}_i = w_1 + \frac{w_2}{1 + e^{-\delta_1(k-\theta_1)}} - \frac{w_3}{1 + e^{-\delta_2(k-\theta_2)}}, \quad (8)$$

where NDVI_i represents NDVI on the i -th day.

We applied the three phenological extraction methods to NOAA CDR NDVI data spanning 1982 to 2021 to obtain phenological data for the Central Asian region, including key indicators such as SOS, EOS, and LOS. The application of multiple methods aims to enhance the reliability and stability of vegetation phenology data, thereby providing a more accurate representation of overall trends. Subsequently, we reduced the noise interference and further increased the data stability by computing the mean of phenological data extracted using the three methods. Initially, we employ three distinct methods to extract Start of Season, End of Season, and Length of Season, respectively. Subsequently, the results obtained from these three methods are averaged to derive the mean SOS, EOS, and LOS. Our study will be conducted using these averaged values. The selection of this approach is aimed at enhancing the stability and accuracy of the model, ensuring that the results possess a high level of reliability.

2.3.2. Partial Least Squares Path Modeling

Partial Least Squares Path Modeling (PLS-PM) is a correlation-based structural equation modeling (SEM) algorithm. In PLS-PM, the concept of causal relationships is expressed based on linear conditional expectations, aiming to discover the best linear predictive relationships while allowing the use of latent variables to estimate complex causal relationships or prediction models. The PLS-PM consists of two submodels: (1) the external model, which associates observed variables with their corresponding latent variables, and (2) the internal model, which links certain latent variables to other latent variables. Four latent variables were defined: vegetation phenology, meteorological factors, topography, and

greenhouse gas levels. The observed variables corresponding to vegetation phenology were SOS, EOS, and LOS. Meteorological factors included temperature, precipitation, SM, and VPD. Topographic factors and greenhouse gases included slope, aspect, elevation, carbon dioxide, nitrous oxide, and methane, respectively.

The relationship between the observed variable (X_{mn}) and the latent variable (ξ_m) is expressed in Equation (9) [34]:

$$X_{mn} = \lambda_{mn}\xi_m + \varepsilon_{mn}, \quad (9)$$

where λ_{mn} denotes the correlation, also known as the loading, between the m -th observed variable in the n -th block and the latent variable. ε_{mn} represents the measurement error term, accounting for inaccuracies in the measurements.

The relationship between latent variables ξ_j is defined by Equation (10):

$$\xi_j = \sum_{i \neq j} \beta_{ji}\xi_i + \zeta_j, \quad (10)$$

Here, ξ_j represents a general endogenous latent variable, β_{ji} is the direct path coefficient from the i -th exogenous latent variable to the j -th endogenous latent variable, and ζ_j signifies the error in the internal model relationships. The calculation of indirect effect coefficients is based on the product of direct path coefficients.

The present study employs the Goodness of Fit (GOF) metric to assess and ascertain the predictive capabilities of the model [35]. GOF is computed using Equation (11):

$$GOF = \sqrt{\text{Communality} \times R^2}, \quad (11)$$

In the formula, GOF is the geometric mean of the community index mean and the R^2 (coefficient of determination) mean. GOF greater than or equal to 0.36 indicates a strong overall fit of the model.

2.4. Statistical Analysis

Initially, we computed the annual mean values of SOS, LOS, and EOS raster images for the Central Asian arid region spanning from 1982 to 2021. Employing univariate linear regression analysis, respectively, we derived the slopes for the average SOS, LOS, and EOS over the past four decades. These slopes were utilized to scrutinize the interannual trends in SOS, LOS, and EOS over multiple years. We also utilized the Mann–Kendall method, a common nonparametric statistical test, to assess the statistical significance of the trend data. Utilizing a multiple linear regression model, calculate the sensitivity of meteorological factors in the Central Asian region to vegetation phenology. In the multiple linear regression model, the regression coefficients for each meteorological factor indicate the degree of impact on vegetation phenology. The positive or negative sign denotes the direction of the impact, while the magnitude of the coefficient signifies the strength of the influence. Larger coefficients imply a more significant impact on vegetation phenology. Based on partial correlation analysis, we examined the relationships between vegetation phenology (including SOS, LOS, and EOS) and meteorological factors (temperature, precipitation, VPD, and SM). This analytical method enabled us to eliminate interferences from other factors, allowing for a more precise exploration of the associations between vegetation phenology and individual meteorological components. By using an SEM approach without latent variables, we studied the effects of meteorological factors on vegetation phenology. The PLS-PM model analyzed the direct, indirect, and overall effects of climate, greenhouse gases, topography, and other latent factors on vegetation phenology.

3. Results

3.1. Spatiotemporal Pattern Analysis of Vegetation Phenology in Central Asia

The correlation coefficient (R^2) between the average SOS values inferred by the three methods and the ground-observed SOS was 0.67, with a significance level of $p < 0.01$ (Figure S1). Hence, the Start of Season (SOS) extracted through remote sensing provides a more accurate reflection of the actual conditions in Central Asia. In the arid region of Central Asia, the SOS is primarily concentrated between 90 and 130 days (comprising 72.26% of the study area). We observed a spatial distribution pattern in which the SOS occurred earlier in the southwest and later in the eastern and northern regions (Figure 2a). Significantly earlier regions (25.29%) were detected in the southern Tianshan Mountains, eastern Kazakhstan, and central Kyrgyzstan. Significantly delayed regions (1.35%) were situated in the northern part of the Tianshan Mountains in Xinjiang and the southern region of Uzbekistan (Figure 2d). The EOS in Central Asia was mainly concentrated between 260 and 300 days (comprising 86.01% of the study area). Based on the observed pattern, the EOS occurs later in the central region and earlier in northern and southern areas (see Figure 2b). Significantly earlier regions (13.52%) were located in southeastern Kazakhstan, and significantly delayed regions (2.98%) were distributed in northern Xinjiang and southern Tajikistan (see Figure 2e). The LOS in Central Asia was primarily concentrated between 140 and 180 days (77.44% of the study area). This shows a spatial distribution pattern with a longer LOS in the central region and a shorter LOS in the northern and southern regions (Figure 2c). Significantly earlier regions (6.03%) were detected in Tajikistan, whereas significantly delayed regions (10.21%) were observed in northern Xinjiang, southern Tajikistan, Kyrgyzstan, and sporadically in northern Kazakhstan (Figure 2f).

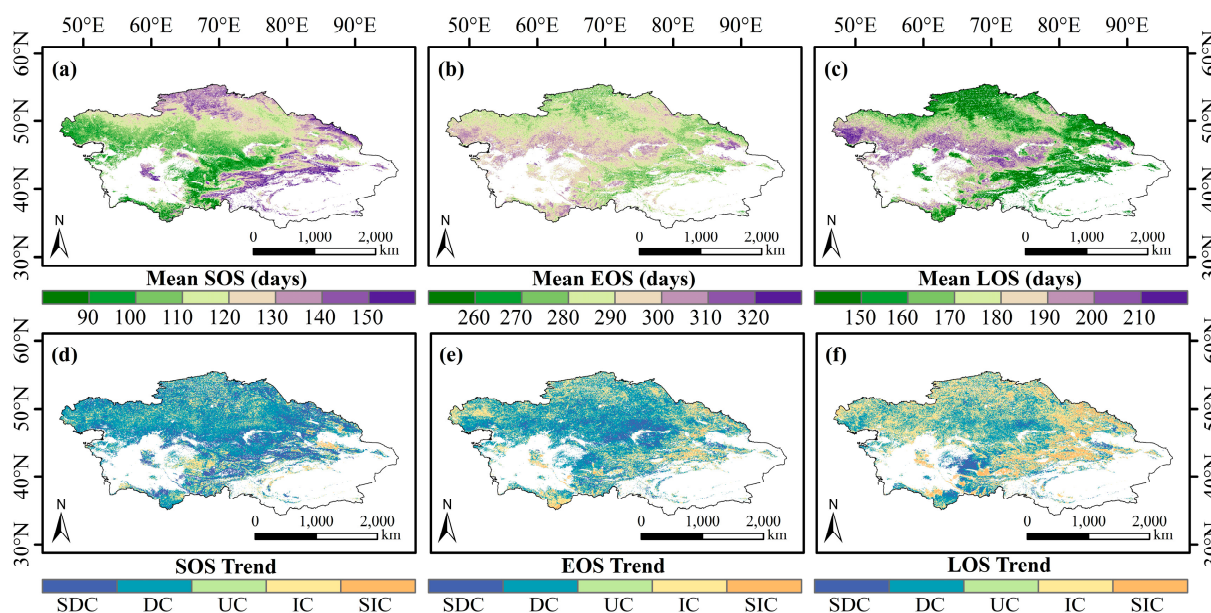


Figure 2. Spatial distribution of the mean and trend in Central Asia for SOS, EOS, and LOS. (a–c) are the mean spatial distributions of SOS, EOS and LOS in recent 40 years, respectively; (d–f) are the spatial variation trends of SOS, EOS and LOS, respectively.

We observed significant interannual trends in vegetation phenology from 1982 to 2021. On average, the SOS decreased by 0.239 days per year, LOS increased by 0.044 days per year, and EOS decreased by 0.125 days per year (Figure 3). These trends indicate that the start and end times of the seasons significantly advanced throughout the study period, whereas the duration of the seasons increased.

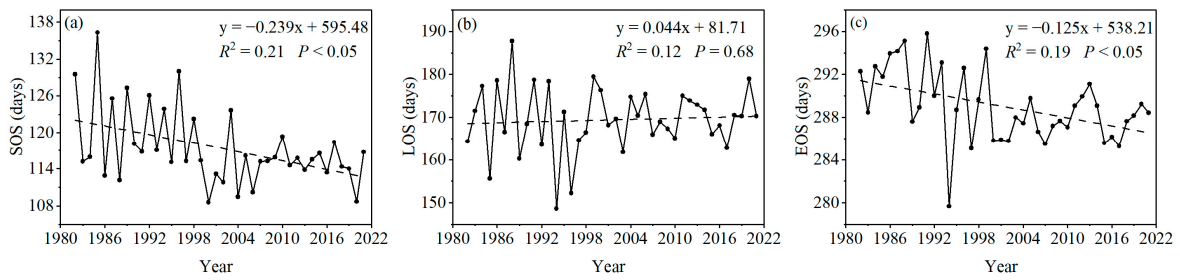


Figure 3. Interannual variations of SOS, EOS, and LOS in Central Asia for the years 1982–2021. (a–c) are the interannual variation trends of SOS, LOS and EOS, respectively.

3.2. Correlations between Meteorological Factors and Vegetation Phenology in Central Asia

The correlation between the SOS and temperature exhibits an overall inverse trend (constituting 80.74% of the entire region). Notably, negative correlations (accounting for 25.53%) were predominantly manifested in the western and southern regions of Kazakhstan and Kyrgyzstan (Figure 4a). The spatial heterogeneity of the partial correlation between the SOS and precipitation is striking. Regions displaying a significant negative correlation (7.20%) were primarily located in southern Kazakhstan and Turkmenistan. Conversely, areas exhibiting a significant positive correlation (3.64%) were primarily concentrated in the northwestern and southeastern parts of the study area (Figure 4b). Regions exhibiting a prominent positive correlation (5.04%) between the SOS and SM were predominantly concentrated in the central sector of the study area. Conversely, noteworthy negative correlations (6.19%) were primarily observed in the southeastern section of the research domain, as illustrated in Figure 4c. Overall, an inverse correlation was observed between the SOS and VPD, which accounted for 65.48% of the entire region. Notably, negative correlations (13.69%) were predominantly distributed in the northern regions of Kazakhstan, encompassing the Altai and Tien Shan mountain ranges. Areas exhibiting a significant positive correlation (2.06%) were mainly located in southwestern Kazakhstan (Figure 4d).

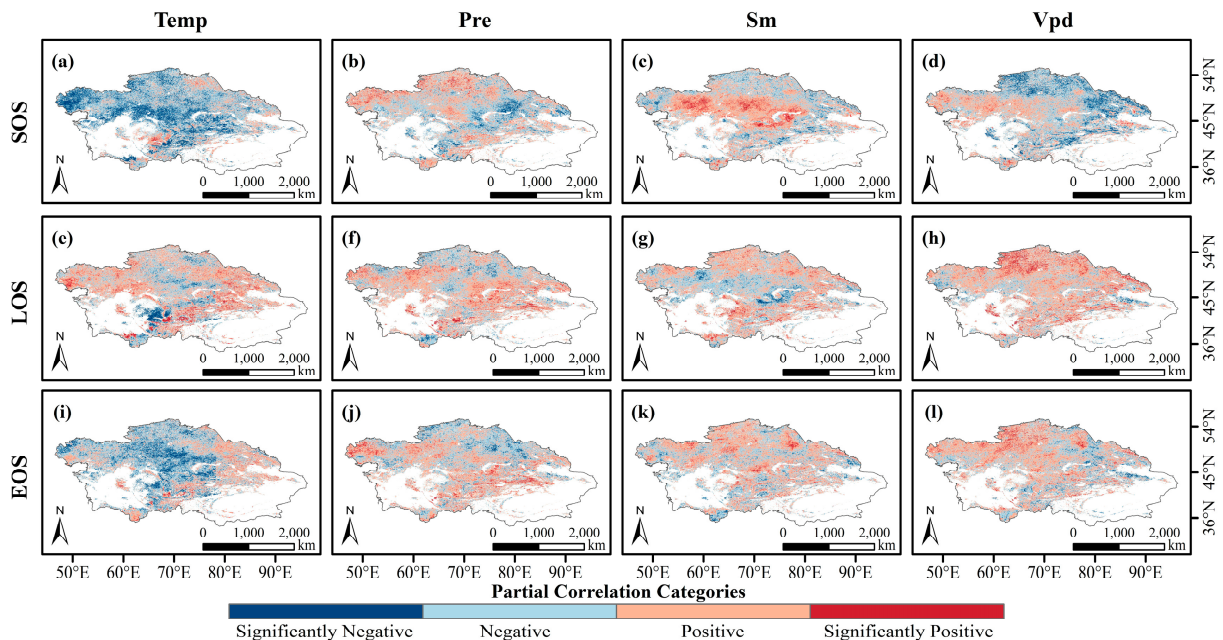


Figure 4. Spatial distribution of partial correlation coefficients between vegetation phenology in Central Asia and temperature, precipitation, soil moisture, and vapor pressure deficit. (a–l) are the spatial distribution of partial correlation coefficients of temperature, precipitation, soil moisture, and vapor pressure deficit with SOS, EOS, and LOS, respectively.

Regions prominently characterized by a significant positive correlation (7.89%) between LOS and temperature were mainly distributed in the northern regions of Kazakhstan and high-altitude mountainous areas (Figure 4e). In contrast, regions marked by a notable negative correlation (6.37%) between the LOS and precipitation were mainly situated in the central parts of Kazakhstan and within the Zhuigeer Basin (Figure 4f). LOS exhibited a substantial positive correlation (4.51%) with SM, which was primarily observed in the northern regions of Kazakhstan and Kyrgyzstan (Figure 4g). Overall, a positive correlation was detected between the LOS and VPD, encompassing 63.08% of the entire region. Regions displaying a notable positive correlation (9.67%) were predominantly located in northern Kazakhstan and northern Xinjiang (Figure 4h).

The correlation between EOS and temperature exhibited an overall negative trend, accounting for 69.34% of the entire region. Negative correlations (16.92%) were primarily observed in Kazakhstan and Uzbekistan (Figure 4i). The EOS demonstrated an overall positive correlation with precipitation, accounting for 51.24% of the entire region. Regions displaying a significant positive correlation (5.74%) were primarily located in Xinjiang and Uzbekistan (Figure 4g). The EOS exhibited an overall positive correlation with the SM, encompassing 51.71% of the entire region. Notably, positive correlations (4.69%) were predominantly observed in northern Xinjiang and Kazakhstan (Figure 4k). The EOS displayed an overall positive correlation with the VPD, accounting for 54.48% of the entire region. Notably, positive correlations (6.13%) were primarily concentrated in northwestern Kazakhstan (Figure 4l).

3.3. Sensitivity of Meteorological Factors to Vegetation Phenology in Central Asia

An increase in temperature by 1 °C resulted in an advancement of 0.34 days in the SOS. Among the pixels, 89.60% exhibited negative sensitivity of SOS to temperature, with a sensitivity range spanning from -5 to 0 days/°C, covering 54.90% of the pixel area (Figure 5a). Every 100 mm increase in annual precipitation led to an advancement of 0.18 days in the SOS. Among the pixels, 55.41% demonstrated a negative sensitivity of SOS to precipitation, with 45.58% of pixels falling within a sensitivity range of -0.5 to 0 days/mm and 30.42% of pixels within the range of 0 to 0.05 days/mm (Figure 5b). Each increment of 0.01 in the SM content led to an advancement of 0.03 days in the SOS. Among the pixels, 74.57% exhibited a positive sensitivity to SM, and 50.46% of these pixels displayed a sensitivity range exceeding 100 days/0.01 SM content (Figure 5c). The effect of atmospheric aridity on the SOS revealed that 84.59% of the pixels exhibited a negative sensitivity of the SOS to atmospheric aridity. The sensitivity range falls between -5 and 0 days/kPa, covering 49.04% of the pixels (Figure 5d).

An increase in temperature by 1 °C resulted in an extension of the LOS by 0.34 days. Among the pixels, 84.59% exhibited a positive sensitivity of LOS to temperature, with a sensitivity range spanning from 0 to 5 days/°C, covering 34.28% of the total pixels (Figure 5e). Regarding precipitation, every 100 mm increase in the annual precipitation led to an advancement of 0.18 days in the LOS. Among the pixels, 53.49% demonstrated a negative sensitivity of LOS to precipitation, with 19.05% of pixels falling within a sensitivity range of -0.5 to 0 days/mm and 17.52% of pixels falling within the range of 0 to 0.05 days/mm (Figure 5f). Each increment of 0.01 in the SM content resulted in an extension of the LOS by 0.03 days. Among the pixels, 62.27% displayed a negative sensitivity of LOS to SM, and 47.88% of these pixels had a sensitivity range smaller than -100 days/0.01 SM content (Figure 5g). The effect of atmospheric aridity on the LOS revealed that 67.10% of the pixels exhibited a positive sensitivity of the LOS to atmospheric aridity. The sensitivity ranged between 0 and 10 days/kPa, covering 51.06% of the pixels (Figure 5h).

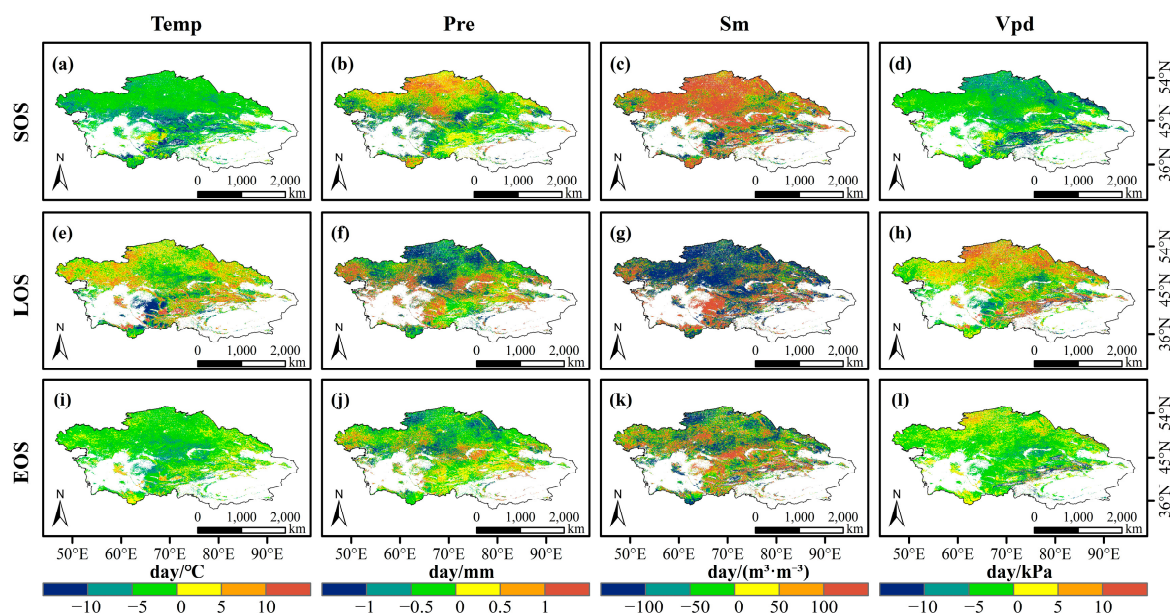


Figure 5. Spatial distribution of the sensitivity of vegetation phenology to temperature, precipitation, soil moisture, and vapor pressure deficit. (a–l) are the spatial distribution of multiple regression coefficients of temperature, precipitation, soil moisture, and vapor pressure deficit and SOS, LOS, and EOS, respectively.

An increase in the temperature by 1°C resulted in an advancement of 0.34 days in the EOS. Among the pixels, 70.67% exhibited a negative sensitivity of EOS to temperature, with a sensitivity range spanning from -5 to 0 days/ $^{\circ}\text{C}$, covering 56.36% of the pixel area (Figure 5i). Regarding precipitation, every 100 mm increase in the annual precipitation led to an advancement of 0.18 days in the EOS. Among the pixels, 54.59% demonstrated a negative sensitivity of EOS to precipitation, with 32.07% and 28.81% of the pixels falling within a sensitivity range of -0.5 to 0 and 0 to 0.05 days/mm, respectively (Figure 5j). Each increment of 0.01 in the SM content led to an extension of 0.03 days in the EOS. Among the pixels, 52.07% exhibited a positive sensitivity of the EOS to SM, with 28.39% of these pixels having a sensitivity range between 0 and 100 days/ 0.01 SM content (Figure 5k). The effect of atmospheric aridity on the EOS revealed that 57.89% of the pixels exhibited a positive sensitivity of the EOS to atmospheric aridity. The sensitivity range was between 0 and 10 days/kPa, covering 41.93% of the pixels (Figure 5l).

The path coefficient results indicate that temperature has a significant effect on SOS, LOS, and EOS, with coefficients of -0.423 , 0.106 , and -0.353 , respectively (Figure 6). For the SOS, the ranking of path coefficient values (in absolute terms) for climatic factors was as follows: $T > \text{precipitation} > \text{VPD} > \text{SM}$. This implies that temperature and precipitation had the most substantial effects on the SOS, whereas soil moisture had the smallest effect. Similarly, for LOS, the ranking of path coefficient values (in absolute terms) for climatic factors was $\text{VPD} > T > \text{precipitation} > \text{SM}$. This indicates that VPD had the most significant effect on LOS, whereas SM had the smallest effect. In the case of the EOS, the ranking of path coefficient values (in absolute terms) for the climatic factors was as follows: $T > \text{VPD} > \text{precipitation} > \text{SM}$. This suggests that the temperature had the most significant effect on EOS, whereas SM had the smallest effect. These results highlight the dominant role of temperature in influencing the spatiotemporal variation in vegetation phenology in Central Asia. However, it is essential to acknowledge that the effects of precipitation and VPD on phenology are equally significant and should not be disregarded.

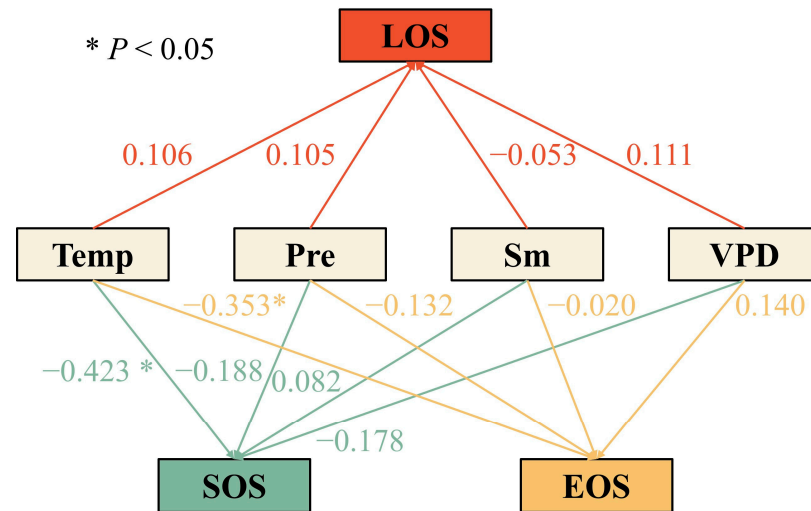


Figure 6. Path analysis of effects of meteorological factors on interannual phenological indicators.

3.4. Research on the Effects of Topographic Factors on Vegetation Phenology in Central Asia

As the elevation gradually increased, the vegetation phenology changed. Significant differences were observed in the phenological trends at different elevations (Figure 7a,d,g). With increasing elevation, the SOS was delayed and the LOS shortened. However, at elevations below 3000 m, an advancing trend of the EOS with increasing elevation was observed. In contrast, at elevations ranging from 3000 to 4000 m, the EOS experienced a delay. Furthermore, the absolute values of the partial correlation coefficients between SOS, LOS, and VPD and elevation showed the most significant associations, whereas EOS had the highest absolute values of the partial correlation coefficients with SM (Figure 8b). This indicates that elevation primarily regulates phenological changes in vegetation by influencing VPD and SM.

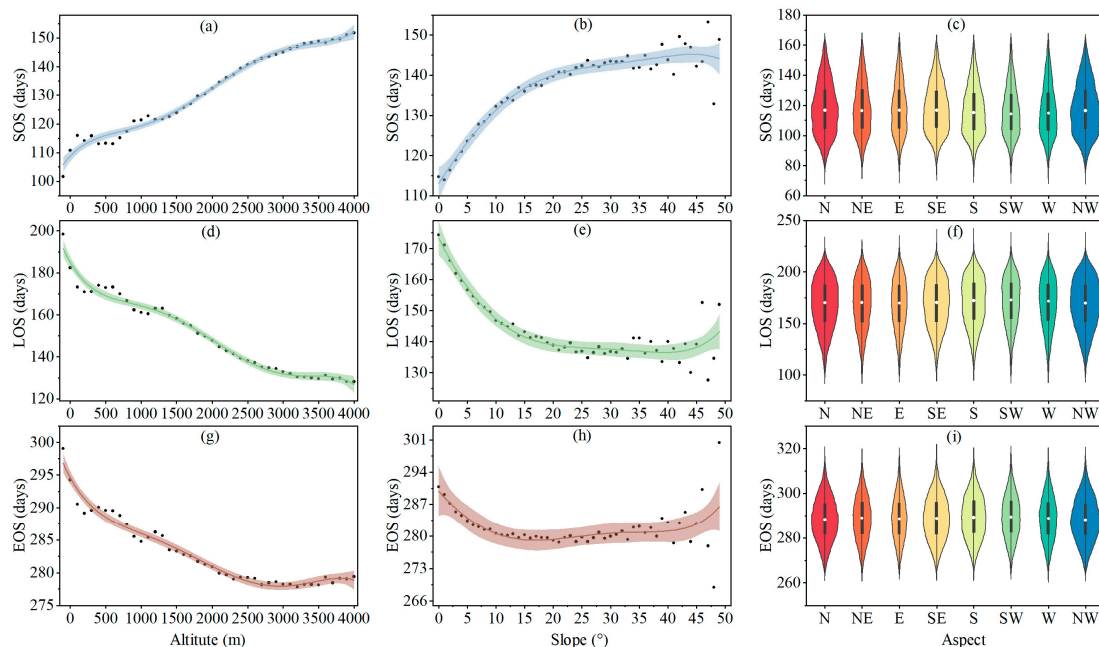


Figure 7. Changes in the vegetation phenology with altitude, slope, and aspect in arid areas of Central Asia. The shadow area represents the 95% confidence interval of the fitted curve. (a–c) are the changes of SOS with altitude, slope and slope direction, respectively. (d–f) are the changes of LOS with elevation, slope and slope direction, respectively. (g–i) are the changes of EOS with altitude, slope and slope direction, respectively.

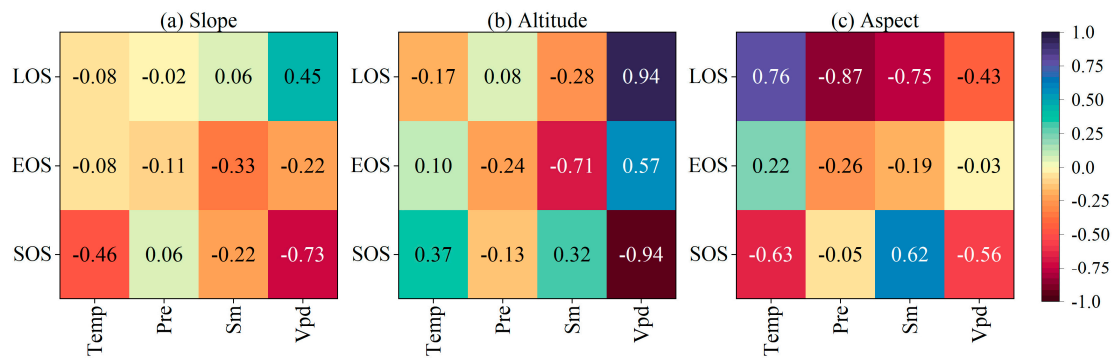


Figure 8. Partial correlation coefficients between phenology and meteorological factors in the arid region of Central Asia under different terrain gradients.

With increasing slope, the vegetation phenology exhibited diverse trends (Figure 7b,e,h). Noticeable differences were observed in the phenological trends of various slopes. Within the slope range of 0° – 25° , the SOS was delayed as the slope increased. However, beyond a slope of 25° , a minimal SOS change was observed. Within the slope range of 0° – 20° , an increase in slope led to a delay in the SOS, an advance in EOS, and a reduction in LOS. However, at slopes greater than 20° , correlations between the EOS, LOS, and slope became less apparent. Furthermore, the absolute values of the partial correlation coefficients between SOS, LOS, and VPD exhibited the most significant association with the slope, whereas EOS displayed the highest absolute partial correlation coefficient with the SM (Figure 8a). This suggests that slopes primarily regulate phenological changes in vegetation by influencing VPD and SM.

The SOS gradually advanced from north, northeast, east, and southeast to south, whereas the EOS and LOS exhibited delayed and prolonged trends in these directions (Figure 7c,f,i). On the other hand, the SOS experienced delays in the southwestern, western, and northwestern directions, whereas the EOS and LOS exhibited advancing and shortening trends in these slope directions. Furthermore, the absolute values of the partial correlation coefficients between SOS, EOS, LOS, and Pre displayed the most significant association in the slope direction, whereas EOS had the highest absolute values of the partial correlation coefficients with the lowest temperature (Figure 8c). This suggests that the slope direction primarily influences vegetation phenological changes by affecting precipitation and temperature.

3.5. Analysis of the Impact Mechanisms of Temporal and Spatial Changes on Vegetation Phenology in Central Asia

The direct effects of climate, topography, and greenhouse gases on phenological factors were determined to be -0.522 , -0.200 , and -0.066 , respectively (Figure 9). Topographic factors indirectly affect phenological factors by influencing greenhouse gases and climatic factors (-0.283). The overall effect, considering both the direct and indirect effects, was -0.483 . Greenhouse gases indirectly affect phenological factors by influencing climatic factors, with a value of 0.027 . The overall effect, considering both the direct and indirect effects, was -0.039 . This suggests that climate change is the primary factor influencing interannual phenological changes. Furthermore, notably high correlation coefficients (absolute values) were obtained between SOS, LOS, temperature, and VPD. In addition, the correlation coefficient between the EOS and VPD was significantly high, as shown in Figure 10. Hence, climate change primarily affects interannual phenological changes through variations in temperature and VPD. Significantly high correlation coefficients (in absolute values) were obtained between SOS, LOS, and EOS with respect to elevation and slope. This indicates that, in the context of climate change, elevation and slope are the primary factors influencing changes in interannual phenological indicators. Significant correlations were observed among SOS, CO_2 , and N_2O , whereas LOS was significantly correlated with N_2O . This suggests that CO_2 and N_2O notably affect the SOS, whereas

N₂O has a significant influence on the LOS. Changes in greenhouse gases did not have a significant effect on the EOS.

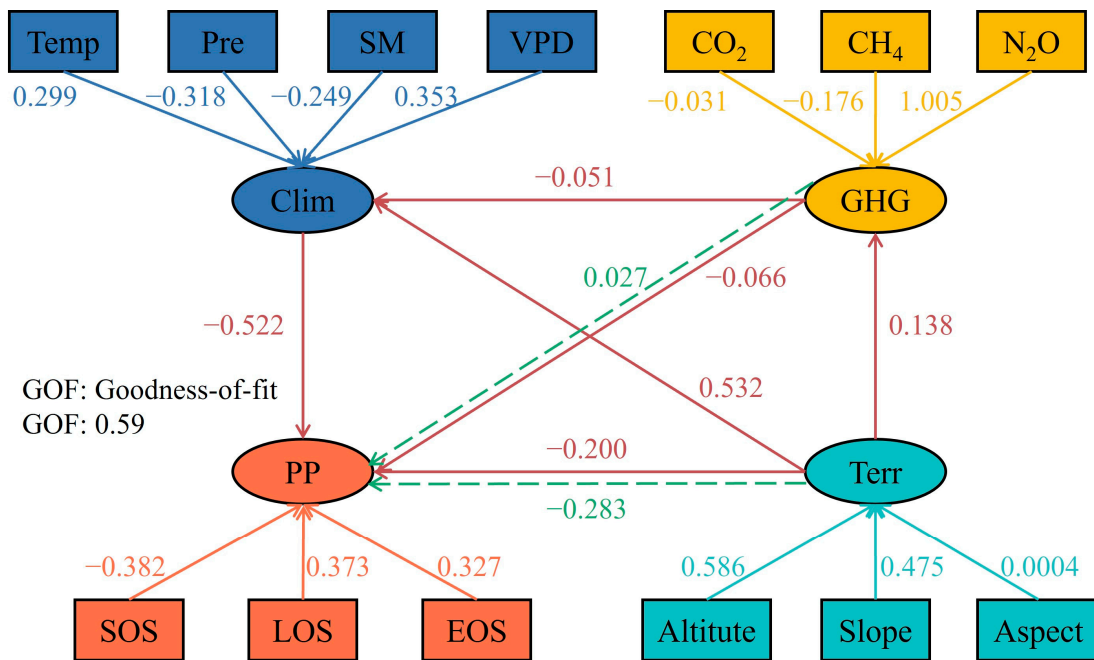


Figure 9. Phenological driving factors were analyzed using the PLS-PM model. Latent variables (LV), observed variables (MV), and connections between MV and their corresponding LV as connections between the LVs are represented by circles, rectangles, and arrows, respectively. Labels on arrows indicate the coefficients of these connections. Solid and dashed arrows represent direct and indirect influences, respectively.

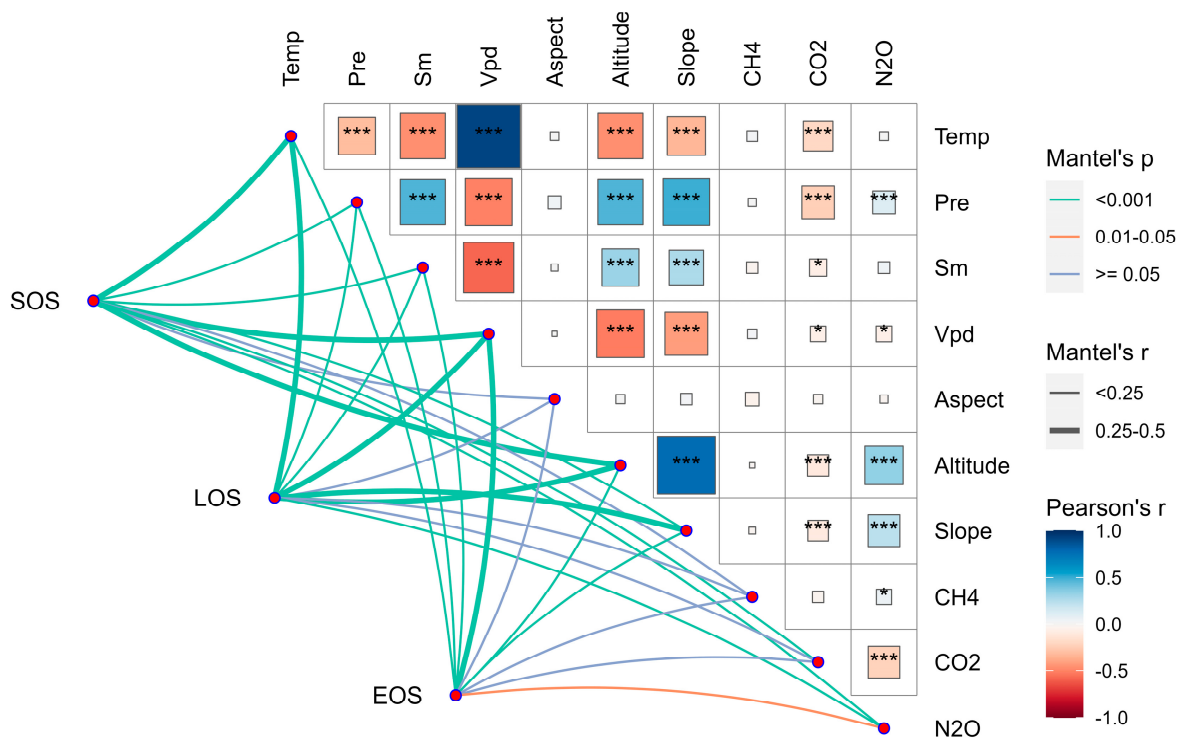


Figure 10. Pearson correlation coefficient analysis assessed correlations between phenological and driving factors. Significance levels are indicated using asterisks (* $p < 0.1$, ** $p < 0.05$, and *** $p < 0.01$).

4. Discussion

4.1. Effect of Climate Change on Vegetation Phenology

In this study, the effect of climate change on vegetation phenology in Central Asia was investigated. The results indicate that the SOS and temperature are significantly negatively correlated. Higher temperatures accelerate heat accumulation, enabling temperatures to rapidly reach the critical threshold required for plant growth [36]. Furthermore, higher temperatures prevent the damage to plants caused by freezing, prompting them to enter their growth states earlier [37]. The correlation between precipitation and vegetation phenology in Central Asia is spatially heterogeneous. A negative correlation was observed between precipitation and SOS in southern Kazakhstan and Turkmenistan. Increased precipitation can provide more water necessary for vegetation growth, prompting plants to enter the growth state earlier, resulting in the advancement of the SOS. In the northwestern and southeastern regions of the study area, SOS and precipitation were positively correlated [38]. The northwestern and southeastern regions are mountainous. While an apparent increase in precipitation may seem favorable for vegetation, the fact that this precipitation occurs over a very short period can potentially lead to severe soil erosion and runoff, damaging plant roots and growth environments. Under such circumstances, the SOS may be delayed because plants require time to adapt and recover from the damage caused by soil erosion and other adverse effects [39]. Compared with precipitation, SM reflects the available water status of plants more directly [40]. We detected a significant positive correlation between SM in Central Asia and the SOS, which differs from previous research, suggesting that SM mitigates drought and advances the SOS [13]. An increase in SM may result in an adjustment of the plant-growing season. Typically, plants commence growth when they have sufficient water. Hence, an increase in SM may delay the onset of the spring growing season because plants no longer need to grow rapidly to adapt to dry conditions [41]. Furthermore, using a SEM, temperature was determined to be the primary factor affecting the SOS. The increase in SM may offset the positive effects of temperature and light on SOS; thus, more sunlight and a rise in temperature might be required to trigger plants to enter a new growth phase [42,43].

VPD is primarily positively correlated with LOS, and its influence on LOS is greater than that of the other meteorological factors. This suggests that the VPD may be one of the main meteorological factors affecting the LOS. An increase in VPD can lead to an increase in leaf transpiration rates because a higher VPD can prompt plants to open their stomata to release excess water vapor to compensate for water evaporation [44]. Although other meteorological factors, such as temperature and precipitation, may also affect the LOS, the influence of VPD is more significant. This positive correlation implies that plants respond to drought and water stress. When the VPD increases, plants respond to drier conditions by extending the LOS to maintain their moisture and growth [45]. This process is crucial for plant survival under drought conditions. In addition, research has shown that an increase in the LOS due to drought does not necessarily enhance vegetation productivity [46].

Temperature plays a dominant role in regulating the EOS, with higher temperatures causing the EOS to advance. Increases in temperature can affect photosynthesis and the decomposition of chlorophyll, which is also related to changes in the leaf color in autumn [47]. At higher temperatures, chlorophyll decomposition accelerates, revealing other pigments in the leaves that cause them to turn yellow, orange, or red. Higher temperatures may cause plants to enter dormancy earlier, resulting in an earlier EOS occurrence [48].

Our results reveal that the LOS is more sensitive to climatic factors (temperature, precipitation, VPD, and SM) than the SOS and EOS. Furthermore, compared with SOS and EOS, the spatial heterogeneity of the effects of climatic factors on LOS is more complex. The LOS is generally highly sensitive to changes in various climatic factors, including temperature, humidity, VPD, and SM. These factors directly affect the opening and closing of plant stomata and transpiration rates and have a significant influence on the entire growth season. In contrast, the SOS and EOS are typically more controlled by factors such

as temperature and precipitation, and their responses may not be as diverse as those of the LOS. Furthermore, LOS may be more sensitive to the physiological and ecological processes of plants because it involves plant water and gas exchange. The LOS is crucial for the functionality of ecosystems because it directly influences water and energy exchange processes [49].

4.2. Effect of the Terrain on Vegetation Phenology

The results of this study show that topographical factors (elevation, slope, and aspect) significantly affect the vegetation phenology in Central Asia. With increasing elevation, the SOS is delayed, and the LOS shortens. The phenological trends of EOS vary at different elevations.

The delay in SOS and shortening of the LOS with increasing elevation occur for the following reasons: As elevation increases, temperatures typically decrease. Areas at higher elevations are generally colder, leading to lower soil temperatures that delay the initiation of plant growth [50]. In high-elevation areas, the duration of snow cover may be longer, and snow cover may inhibit plant growth. High-elevation regions may also experience shorter daylight hours because mountainous terrain obstructs sunlight [51]. This results in less sunlight being received by plants per day, thereby delaying the start of the growing season. High-elevation areas often have poor soil conditions, such as infertile and poorly drained soils, which can limit the growth rate of plants. Therefore, the SOS occurs relatively later, and LOS is relatively shorter because plants require more time to adapt to these unfavorable conditions. The influence of elevation on EOS often exhibits different trends. Below an elevation of 3000 m, the earlier EOS may be due to a decrease in temperature. Areas at lower elevations are generally warmer, and a decrease in temperature can accelerate the end of the plant-growing season, resulting in an earlier EOS [52]. Precipitation patterns may also influence the EOS. Some areas at lower elevations might have distinct dry seasons, and a decrease in precipitation could lead to an earlier end of the plant-growing season. At elevations ranging from 3000 to 4000 m, the delay in the EOS may be due to regions at higher elevations accumulating more snow. Snow cover continues to reflect sunlight and maintain relatively low temperatures [53]. Lower temperatures might slow plant growth and the process of leaf color change, leading to a relatively later appearance of autumn phenology. Additionally, high-elevation areas may experience shorter daylight hours, resulting in insufficient sunlight and delayed plant growth and leaf color change [54]. Elevation primarily regulates phenological changes in vegetation by affecting the VPD and SM (Figure 8b). With increasing elevation, the atmosphere is typically thinner, and the temperature and humidity may decrease. Lower atmospheric pressure and humidity can influence changes in the VPD. Higher elevations, which often have lower VPDs, help vegetation maintain moisture because of lower evaporation rates. This may lead to slower phenological processes, such as flowering and leaf color changes [55]. Increased elevation also influences the availability of SM. Higher altitudes are typically characterized by a greater accumulation of snow and ice during colder seasons, prolonging the thawing and melting processes of the soil. This phenomenon may lead to a delayed release of SM in spring, consequently affecting the phenological changes of vegetation and resulting in a delayed occurrence thereof [56].

Augmentation of slope inclination results in the postponement of the SOS. This can be attributed to the steeper nature of these slopes, where the angle of solar irradiation is relatively shallow, potentially yielding lower ground temperatures. This, in turn, retards the vernal reawakening of vegetation. Vegetation requires a protracted duration to acclimatize to diminished temperatures and reduced solar exposure, thus resulting in a delay in the SOS [57]. Conversely, an increase in the slope inclination may induce the advancement of the EOS. On steeper slopes, the solar angle of incidence becomes more acute, resulting in a swifter temperature increase. Consequently, vegetation may enter dormancy earlier, leading to the premature occurrence of EOS [58].

Aspect primarily influences vegetation phenology through its effects on precipitation and temperature. Aspect can significantly modulate the precipitation distribution. In

Central Asia, north-facing slopes tend to be warmer because they are sunward-oriented; thus, they absorb a greater amount of solar radiation. In contrast, south-facing slopes typically remain cooler because they are sun-averse and have diminished solar exposure. This disparity may result in reduced precipitation on north-facing slopes and increased precipitation on south-facing slopes [59]. This divergence in precipitation may affect the water supply to vegetation, consequently influencing its phenology. This also influences the temperature distribution. The orientation of the slope governs the direct angle of solar incidence on the ground. South-facing slopes are more prone to direct solar exposure during the day, resulting in elevated soil and surface temperatures. Conversely, north-facing slopes receive comparatively less solar radiation, leading to lower temperatures. This temperature differential can influence the rate of vegetation growth and development as well as the timing of phenological events.

4.3. Effects of Climate, Terrain, and Greenhouse Gases on Vegetation Phenology

Conducting a PLS-PM path analysis to assess the integrated impact of climate, topography, and greenhouse gases on vegetation phenology, we discern that climate change stands as the principal factor influencing inter-annual variations in phenological patterns. Climatic factors, including temperature, precipitation, and solar radiation, directly govern vegetation growth and development [60]. The direct influence of climatic factors on vegetation plays a pivotal role in phenology. Climate change is typically accompanied by a global temperature escalation. An increase in temperature leads to early spring warming, prompting plants to initiate their growth seasons sooner. This has resulted in the advancement of phenological events, a trend observed in numerous regions [61]. Climate change has also triggered erratic precipitation patterns, including droughts and uneven rainfall. These irregular precipitation patterns directly affect the water supply to vegetation, potentially resulting in irregular and delayed phenological events. Vegetation requires an adequate water supply to sustain growth and flowering; hence, alterations in precipitation patterns significantly influence the phenology [62]. Climate change is a global issue that encompasses the integrated alteration of multiple climatic factors, including temperature, precipitation, and extreme weather events [63]. These factors collectively influence the growth and phenological changes in vegetation, rendering climate change a comprehensive and multifaceted influencing factor. Long-term trends in climatic elements have sustained and cumulative effects on vegetation phenology. As climate change continues, vegetation gradually adapts to new climatic conditions, resulting in a shift in the timing of phenological events. In summary, climate factors encompass the direct effects on vegetation, the warming effect induced by climate change, erratic precipitation patterns, the global and comprehensive nature of climate change, and the long-term trends of climatic elements that converge to establish climate change as the primary driver of interannual vegetation phenological variation. Temperature and VPD strongly correlate with phenology and are among the most pivotal climatic factors. Elevated temperatures foster plant growth, resulting in early spring warming and advanced phenology, whereas lower temperatures may contribute to phenological delays. The VPD, which represents the disparity between the leaf transpiration water demand and moisture requirement of the surrounding air, signifies dry atmospheric conditions. This, in turn, prompts plants to adapt their water-utilization strategies through phenological adjustments. Temperature and VPD directly affect plant growth and phenological events [64]. The strong correlation among these factors underscores their pivotal roles in governing the ecological responses of plants and ecosystem phenology.

Topographic factors affect vegetation phenology that surpass their direct impact through the indirect regulation of greenhouse gases and climatic elements. Mountains induce upward air movement and augment precipitation, whereas valleys are often drier. This divergence in precipitation distribution directly affects vegetation water utilization and availability and consequently significantly influences phenological events. Therefore, topography plays a pivotal role in the allocation of water resources within ecosystems [65].

Topographical gradients give rise to temperature disparities, with high-altitude areas typically being cooler and low-lying regions being warmer. These temperature differences influence the seasonality and rhythm of vegetation growth. High-altitude areas may experience spring at relatively low temperatures, resulting in delayed phenological events, whereas low-lying regions enter spring at higher temperatures, potentially causing early occurrences [66]. Topographic features can alter atmospheric circulation, including wind direction and speed, thereby affecting the distribution and dispersion of greenhouse gases. Mountains and valleys may lead to the accumulation of greenhouse gases in certain areas, subsequently affecting the atmospheric temperature and humidity. Changes in climatic factors directly influence vegetation growth and phenology.

We analyzed the correlation between greenhouse gases and vegetation phenology. The results of this research indicate that CO₂ significantly influences the SOS. Increased CO₂ concentrations may stimulate plant growth and photosynthesis, resulting in the advancement of the plant SOS [67]. The increase in the N₂O content enhances the greenhouse effect in the atmosphere because it has the capacity to absorb and re-emit the Earth's surface infrared radiation, thereby prolonging the retention of heat in the atmosphere. This, in turn, influences the LOS of vegetation [68]. The effects of greenhouse gas changes on the EOS of vegetation are not significant. This may be attributed to the fact that a multitude of climatic and environmental factors, including temperature, precipitation, and solar radiation, influence the EOS. The intricate interplay among these factors may obscure the potential effects of greenhouse gas variations on the EOS. Further research and analysis are required to elucidate the specific reasons for these effects.

Through a comprehensive consideration of temperature, topographical factors, water resource management, climate change adaptation and mitigation measures, research and technological innovation, as well as education and advocacy, one can more effectively address ecological issues in the Central Asian region. This involves achieving efficient utilization of water resources, safeguarding and restoring the stability and sustainable development of arid ecosystems. These integrated measures include: adapting grassland irrigation based on real-time temperature changes to accommodate early plant growth, and reducing irrigation amounts to prevent premature vegetation growth. Selecting vegetation species with strong adaptability based on topographical factors, improving soil drought resistance, and enhancing soil water retention capacity to increase the stability of the vegetation ecosystem. Monitoring and predicting water resources, temperature, and phenological changes, and dynamically adjusting water resource allocation and vegetation management. Promoting low-carbon production methods, reducing greenhouse gas emissions, and researching innovative technologies to understand the impact mechanisms of meteorological factors on vegetation phenology, thereby reducing ecosystem vulnerability. Through educational and advocacy activities, raising public and decision-makers' awareness of water resources and arid ecosystems, fostering public participation, and supporting relevant policies and projects. These comprehensive measures can promote the effective use of water resources and protect and restore the stability and sustainable development of arid ecosystems. Additionally, ongoing research, technological innovation, education, and advocacy are necessary to continually enhance understanding and problem-solving capabilities regarding ecological issues in the Central Asian land ecosystems.

4.4. Uncertainty

This study delves deeply into the comprehensive mechanisms underlying the spatiotemporal effects of climate, topography, and greenhouse gases on vegetation phenology, providing a vital scientific foundation for ecosystem management and climate adaptation. However, this study has certain limitations. First, the effects of seasonal meteorological factors on vegetation phenology were not thoroughly explored. Seasonal meteorological factors, including spring precipitation, high summer temperatures, and autumn droughts, have significant and intricate effects on vegetation phenological events [69]. These seasonal climatic factors may significantly affect vegetation growth and life cycles during specific

seasons. Second, although we considered the integrated effects of climate, topography, and greenhouse gases on vegetation phenology, the focus must be placed on the influence of extreme weather events on phenology. Extreme weather events, such as droughts, floods, and severe winds, may have a more pronounced effect on vegetation phenology, particularly as climate change intensifies [70,71]. Hence, further research on how weather events shape vegetation phenology will contribute to a more comprehensive understanding of vegetation responses to climate change. Future research plans will focus on analyzing the impact of government-implemented sustainable vegetation management, forest resource strategies, human activities, and soil nutrient factors on vegetation phenology. The intention is to propose methods that integrate complex models or technologies to offer more precise and reliable predictions and explanations. This approach aims to enhance the understanding and response to vegetation's reactions to environmental changes. Finally, the validation data mentioned in this study primarily focus on the Xinjiang region, whereas the data measured in other parts of Central Asia are relatively limited. This could limit the overall understanding of phenological changes in vegetation in Central Asia. Future research should include the collection of measured data from a broader range of regions in Central Asia to ensure more representative and credible study results.

5. Conclusions

Previous research predominantly focused on the correlation between Central Asian vegetation phenology and climate change, emphasizing the impact of singular environmental factors on vegetation phenology while disregarding the direct and indirect influence of various factors such as climate, topography, and greenhouse gases on vegetation phenology. In this study, we conducted an in-depth analysis of spatiotemporal changes in Central Asian vegetation phenology from 1982 to 2021 to identify the combined effect of climate, topography, and greenhouse gas variables on vegetation phenology. The results of this study indicate that vegetation phenology exhibited distinct interannual variations from 1982 to 2021. The annual decrease in the average SOS was 0.239 days, the average LOS increased by 0.044 days, and the annual decrease in the average EOS was 0.125 days. Temperature plays a dominant role in spatiotemporal variations of Central Asian vegetation phenology, with each 1 °C rise in temperature leading to an advancement of the SOS by 0.34 days, an extension of the LOS by 0.34 days, and an earlier occurrence of the EOS (by 0.34 days). Furthermore, topographic factors, including elevation, slope, and aspect, also significantly influence vegetation phenological changes. Elevation and slope regulate vegetation phenological variations by affecting VPD and SM, whereas aspect primarily shapes the spatiotemporal patterns of vegetation phenology through its effect on precipitation and temperature. Compared with topography and greenhouse gases, meteorological factors are the dominant environmental factors influencing interannual phenological variations. Temperature and VPD are the principal meteorological factors that profoundly affect the interannual dynamics of vegetation phenology. The findings of this study contribute to deepening our understanding of the integrated response relationships between Central Asian vegetation phenology, climate, topography, and greenhouse gases. It provides crucial scientific foundations for ecosystem restoration and environmental adaptation strategies in the Central Asian region.

Supplementary Materials: The following supporting information can be downloaded at: <https://www.mdpi.com/article/10.3390/land13020180/s1>, Figure S1: The correlation coefficient between the mean SOS values retrieved using three different inversion methods and the SOS observed at the ground level.

Author Contributions: R.T.: Conceptualization, Methodology, Writing–criticism and editing. J.L.: Resources, Formal Analysis, Methodology, Supervision. J.Z.: Writing–reviewing and editing, Visualization, Supervision, Funding. W.H.: Methodology, Resources, Supervision. L.L.: Conceptualization, Software. Y.L.: Methodology, Resources, Supervision. All authors have read and agreed to the published version of the manuscript.

Funding: This study was sponsored by the Study on the Response Mechanism of Grassland Net Primary Productivity to Extreme Drought in Xinjiang (2022D04009).

Data Availability Statement: Data is contained within the article.

Acknowledgments: We thank the Office of the Command of Locust Control and Rodent Eradication in Xinjiang Uygur Autonomous Region, the base for joint industry–university–research postgraduate training, and the Xinjiang General Grassland Station for providing data and field research support.

Conflicts of Interest: The authors declare no conflicts of interest.

References

1. Frappart, F.; Wigneron, J.-P.; Li, X.; Liu, X.; Al-Yaari, A.; Fan, L.; Wang, M.; Moisy, C.; Le Masson, E.; Aoulad Lafkih, Z.; et al. Global Monitoring of the Vegetation Dynamics from the Vegetation Optical Depth (VOD): A Review. *Remote Sens.* **2020**, *12*, 2915. [\[CrossRef\]](#)
2. Yu, L.; Liu, Y.; Li, X.; Yan, F.; Lyne, V.; Liu, T. Vegetation-Induced Asymmetric Diurnal Land Surface Temperatures Changes across Global Climate Zones. *Sci. Total Environ.* **2023**, *896*, 165255. [\[CrossRef\]](#)
3. Cortés, J.; Mahecha, M.D.; Reichstein, M.; Myneni, R.B.; Chen, C.; Brenning, A. Where Are Global Vegetation Greening and Browning Trends Significant? *Geophys. Res. Lett.* **2021**, *48*, e2020GL091496. [\[CrossRef\]](#)
4. Yang, L.; Zhao, S.; Liu, S.J.G.C.B. Urban environments provide new perspectives for forecasting vegetation phenology responses under climate warming. *Glob. Change Biol.* **2023**, *29*, 4383–4396. [\[CrossRef\]](#) [\[PubMed\]](#)
5. Vicca, S. Global Vegetation's CO₂ Uptake. *Nat. Ecol. Evol.* **2018**, *2*, 1840–1841. [\[CrossRef\]](#)
6. Zhang, X.; Liu, M. Topography Regulates the Responses of Water Partitioning to Climate and Vegetation Seasonality. *Sci. Total Environ.* **2022**, *838*, 156028. [\[CrossRef\]](#)
7. Adole, T.; Dash, J.; Rodriguez-Galiano, V.; Atkinson, P.M. Photoperiod Controls Vegetation Phenology across Africa. *Commun. Biol.* **2019**, *2*, 391. [\[CrossRef\]](#)
8. Revermann, R.; Finckh, M.; Stellmes, M.; Strohbach, B.J.; Frantz, D.; Oldeland, J. Linking Land Surface Phenology and Vegetation-Plot Databases to Model Terrestrial Plant α -Diversity of the Okavango Basin. *Remote Sens.* **2016**, *8*, 370. [\[CrossRef\]](#)
9. Li, J.; Guan, J.; Han, W.; Tian, R.; Lu, B.; Yu, D.; Zheng, J. Important Role of Precipitation in Controlling a More Uniform Spring Phenology in the Qinba Mountains, China. *Front. Plant Sci.* **2023**, *14*, 1074405. [\[CrossRef\]](#) [\[PubMed\]](#)
10. Linkosalmi, M.; Tuovinen, J.-P.; Nevalainen, O.; Peltoniemi, M.; Taniš, C.M.; Arslan, A.N.; Rainne, J.; Lohila, A.; Laurila, T.; Aurela, M. Tracking Vegetation Phenology of Pristine Northern Boreal Peatlands by Combining Digital Photography with CO₂ Flux and Remote Sensing Data. *Biogeosciences* **2022**, *19*, 4747–4765. [\[CrossRef\]](#)
11. Zhang, J.; Chen, S.; Wu, Z.; Fu, Y.H. Review of Vegetation Phenology Trends in China in a Changing Climate. *Prog. Phys. Geogr. Earth Environ.* **2022**, *46*, 829–845. [\[CrossRef\]](#)
12. Piao, S.; Friedlingstein, P.; Ciais, P.; Viovy, N.; Demarty, J. Growing Season Extension and Its Impact on Terrestrial Carbon Cycle in the Northern Hemisphere over the Past 2 Decades. *Glob. Biogeochem. Cycles* **2007**, *21*, 2006GB002888. [\[CrossRef\]](#)
13. Luo, M.; Meng, F.; Sa, C.; Duan, Y.; Bao, Y.; Liu, T.; De Maeyer, P. Response of Vegetation Phenology to Soil Moisture Dynamics in the Mongolian Plateau. *CATENA* **2021**, *206*, 105505. [\[CrossRef\]](#)
14. Yang, J.; El-Kassaby, Y.A.; Guan, W. The Effect of Slope Aspect on Vegetation Attributes in a Mountainous Dry Valley, Southwest China. *Sci. Rep.* **2020**, *10*, 16465. [\[CrossRef\]](#) [\[PubMed\]](#)
15. Chen, Z.; Wang, W.; Fu, J. Vegetation Response to Precipitation Anomalies under Different Climatic and Biogeographical Conditions in China. *Sci. Rep.* **2020**, *10*, 830. [\[CrossRef\]](#) [\[PubMed\]](#)
16. Norby, R.J.; Zak, D.R. Ecological Lessons from Free-Air CO₂ Enrichment (FACE) Experiments. *Annu. Rev. Ecol. Evol. Syst.* **2011**, *42*, 181–203. [\[CrossRef\]](#)
17. Liu, X.; Sun, G.; Fu, Z.; Ciais, P.; Feng, X.; Li, J.; Fu, B. Compound Droughts Slow down the Greening of the Earth. *Glob. Chang. Biol.* **2023**, *29*, 3072–3084. [\[CrossRef\]](#)
18. Liu, L.; Peng, J.; Li, G.; Guan, J.; Han, W.; Ju, X.; Zheng, J. Effects of Drought and Climate Factors on Vegetation Dynamics in Central Asia from 1982 to 2020. *J. Environ. Manag.* **2023**, *328*, 116997. [\[CrossRef\]](#) [\[PubMed\]](#)
19. Chen, C.; Zhang, X.; Lu, H.; Jin, L.; Du, Y.; Chen, F. Increasing Summer Precipitation in Arid Central Asia Linked to the Weakening of the East Asian Summer Monsoon in the Recent Decades. *Int. J. Climatol.* **2021**, *41*, 1024–1038. [\[CrossRef\]](#)
20. Hu, Z.; Zhang, C.; Hu, Q.; Tian, H. Temperature Changes in Central Asia from 1979 to 2011 Based on Multiple Datasets. *J. Clim.* **2014**, *27*, 1143–1167. [\[CrossRef\]](#)
21. Zhou, X.; Lv, X.; Tao, Y.; Wu, L.; Havrilla, C.A.; Zhang, Y. Divergent Responses of Nitrous Oxide, Methane and Carbon Dioxide Exchange to Pulses of Nitrogen Addition in a Desert in Central Asia. *CATENA* **2019**, *173*, 29–37. [\[CrossRef\]](#)
22. Li, J.; Chen, X.; Kurban, A.; Van De Voorde, T.; De Maeyer, P.; Zhang, C. Coupled SSPs-RCPs Scenarios to Project the Future Dynamic Variations of Water-Soil-Carbon-Biodiversity Services in Central Asia. *Ecol. Indic.* **2021**, *129*, 107936. [\[CrossRef\]](#)
23. Wu, L.; Ma, X.; Dou, X.; Zhu, J.; Zhao, C. Impacts of Climate Change on Vegetation Phenology and Net Primary Productivity in Arid Central Asia. *Sci. Total Environ.* **2021**, *796*, 149055. [\[CrossRef\]](#)

24. Gao, X.; Zhao, D. Impacts of Climate Change on Vegetation Phenology over the Great Lakes Region of Central Asia from 1982 to 2014. *Sci. Total Environ.* **2022**, *845*, 157227. [[CrossRef](#)] [[PubMed](#)]
25. Liu, L.; Guan, J.; Zheng, J.; Wang, Y.; Han, W.; Liu, Y. Cumulative Effects of Drought Have an Impact on Net Primary Productivity Stability in Central Asian Grasslands. *J. Environ. Manag.* **2023**, *344*, 118734. [[CrossRef](#)] [[PubMed](#)]
26. Yu, Z.; Zhang, Y.; Wang, P.; Yu, J.; Wang, T.; Shi, S. Detection of the Nonlinear Response of Vegetation to Terrestrial Water Storage Changes in Central Asian Endorheic Basins. *Ecol. Indic.* **2023**, *154*, 110901. [[CrossRef](#)]
27. Bindajam, A.A.; Mallick, J.; AlQadhi, S.; Singh, C.K.; Hang, H.T. Impacts of Vegetation and Topography on Land Surface Temperature Variability over the Semi-Arid Mountain Cities of Saudi Arabia. *Atmosphere* **2020**, *11*, 762. [[CrossRef](#)]
28. Chen, J.; Jönsson, P.; Tamura, M.; Gu, Z.; Matsushita, B.; Eklundh, L. A Simple Method for Reconstructing a High-Quality NDVI Time-Series Data Set Based on the Savitzky–Golay Filter. *Remote Sens. Environ.* **2004**, *91*, 332–344. [[CrossRef](#)]
29. White, M.A.; Thornton, P.E.; Running, S.W. A Continental Phenology Model for Monitoring Vegetation Responses to Interannual Climatic Variability. *Glob. Biogeochem. Cycles* **1997**, *11*, 217–234. [[CrossRef](#)]
30. Xue, Y.; Bai, X.; Zhao, C.; Tan, Q.; Li, Y.; Luo, G.; Wu, L.; Chen, F.; Li, C.; Ran, C.; et al. Spring Photosynthetic Phenology of Chinese Vegetation in Response to Climate Change and Its Impact on Net Primary Productivity. *Agric. For. Meteorol.* **2023**, *342*, 109734. [[CrossRef](#)]
31. Mariën, B.; Balzarolo, M.; Dox, I.; Leys, S.; Lorène, M.J.; Geron, C.; Portillo-Estrada, M.; AbdElgawad, H.; Asard, H.; Campioli, M. Detecting the Onset of Autumn Leaf Senescence in Deciduous Forest Trees of the Temperate Zone. *New Phytol.* **2019**, *224*, 166–176. [[CrossRef](#)]
32. Zhang, X.; Friedl, M.A.; Schaaf, C.B.; Strahler, A.H.; Hodges, J.C.F.; Gao, F.; Reed, B.C.; Huete, A. Monitoring Vegetation Phenology Using MODIS. *Remote Sens. Environ.* **2003**, *84*, 471–475. [[CrossRef](#)]
33. Gonsamo, A.; Chen, J.M.; Price, D.T.; Kurz, W.A.; Wu, C. Land Surface Phenology from Optical Satellite Measurement and CO₂ Eddy Covariance Technique. *J. Geophys. Res. Biogeosci.* **2012**, *117*, 2012JG002070. [[CrossRef](#)]
34. Esposito Vinzi, V.; Chin, W.W.; Henseler, J.; Wang, H. (Eds.) *Handbook of Partial Least Squares: Concepts, Methods and Applications*; Springer: Berlin/Heidelberg, Germany, 2010; ISBN 978-3-540-32825-4.
35. Tenenhaus, M.; Vinzi, V.E.; Chatelin, Y.-M.; Lauro, C. PLS Path Modeling. *Comput. Stat. Data Anal.* **2005**, *48*, 159–205. [[CrossRef](#)]
36. Ren, S.; Li, Y.; Peichl, M. Diverse Effects of Climate at Different Times on Grassland Phenology in Mid-Latitude of the Northern Hemisphere. *Ecol. Indic.* **2020**, *113*, 106260. [[CrossRef](#)]
37. Wang, H.; Wu, C.; Ciais, P.; Peñuelas, J.; Dai, J.; Fu, Y.; Ge, Q. Overestimation of the Effect of Climatic Warming on Spring Phenology Due to Misrepresentation of Chilling. *Nat. Commun.* **2020**, *11*, 4945. [[CrossRef](#)] [[PubMed](#)]
38. Cheng, M.; Wang, Y.; Zhu, J.; Pan, Y. Precipitation Dominates the Relative Contributions of Climate Factors to Grasslands Spring Phenology on the Tibetan Plateau. *Remote Sens.* **2022**, *14*, 517. [[CrossRef](#)]
39. Li, P.; Zhu, Q.; Peng, C.; Zhang, J.; Wang, M.; Zhang, J.; Ding, J.; Zhou, X. Change in Autumn Vegetation Phenology and the Climate Controls From 1982 to 2012 on the Qinghai–Tibet Plateau. *Front. Plant Sci.* **2020**, *10*, 1677. [[CrossRef](#)]
40. Koster, R. 13 Corresponding Author Address. Available online: https://journals.ametsoc.org/view/journals/hydr/16/4/jhm-d-14-0205_1.xml (accessed on 28 January 2024).
41. Dang, C.; Shao, Z.; Huang, X.; Zhuang, Q.; Cheng, G.; Qian, J. Vegetation Greenness and Photosynthetic Phenology in Response to Climatic Determinants. *Front. For. Glob. Chang.* **2023**, *6*, 1172220. [[CrossRef](#)]
42. Jin, Z.; Zhuang, Q.; He, J.-S.; Luo, T.; Shi, Y. Phenology Shift from 1989 to 2008 on the Tibetan Plateau: An Analysis with a Process-Based Soil Physical Model and Remote Sensing Data. *Clim. Chang.* **2013**, *119*, 435–449. [[CrossRef](#)]
43. Yang, X.; Hao, Y.; Cao, W.; Yu, X.; Hua, L.; Liu, X.; Yu, T.; Chen, C. How Does Spring Phenology Respond to Climate Change in Ecologically Fragile Grassland? A Case Study from the Northeast Qinghai–Tibet Plateau. *Sustainability* **2021**, *13*, 12781. [[CrossRef](#)]
44. Li, S.; Wang, G.; Chai, Y.; Miao, L.; Fifi Tawia Hagan, D.; Sun, S.; Huang, J.; Su, B.; Jiang, T.; Chen, T.; et al. Increasing Vapor Pressure Deficit Accelerates Land Drying. *J. Hydrol.* **2023**, *625*, 130062. [[CrossRef](#)]
45. Cheng, Y.; Liu, L.; Cheng, L.; Fa, K.; Liu, X.; Huo, Z.; Huang, G. A Shift in the Dominant Role of Atmospheric Vapor Pressure Deficit and Soil Moisture on Vegetation Greening in China. *J. Hydrol.* **2022**, *615*, 128680. [[CrossRef](#)]
46. Ge, W.; Han, J.; Zhang, D.; Wang, F. Divergent Impacts of Droughts on Vegetation Phenology and Productivity in the Yungui Plateau, Southwest China. *Ecol. Indic.* **2021**, *127*, 107743. [[CrossRef](#)]
47. Ma, R.; Shen, X.; Zhang, J.; Xia, C.; Liu, Y.; Wu, L.; Wang, Y.; Jiang, M.; Lu, X. Variation of Vegetation Autumn Phenology and Its Climatic Drivers in Temperate Grasslands of China. *Int. J. Appl. Earth Obs. Geoinf.* **2022**, *114*, 103064. [[CrossRef](#)]
48. Li, P.; Liu, Z.; Zhou, X.; Xie, B.; Li, Z.; Luo, Y.; Zhu, Q.; Peng, C. Combined Control of Multiple Extreme Climate Stressors on Autumn Vegetation Phenology on the Tibetan Plateau under Past and Future Climate Change. *Agric. For. Meteorol.* **2021**, *308–309*, 108571. [[CrossRef](#)]
49. Zhong, R.; Yan, K.; Gao, S.; Yang, K.; Zhao, S.; Ma, X.; Zhu, P.; Fan, L.; Yin, G. Response of Grassland Growing Season Length to Extreme Climatic Events on the Qinghai–Tibetan Plateau. *Sci. Total Environ.* **2024**, *909*, 168488. [[CrossRef](#)] [[PubMed](#)]
50. Gong, H.; Cheng, Q.; Jin, H.; Ren, Y. Effects of Temporal, Spatial, and Elevational Variation in Bioclimatic Indices on the NDVI of Different Vegetation Types in Southwest China. *Ecol. Indic.* **2023**, *154*, 110499. [[CrossRef](#)]
51. Zhang, L.; Shen, M.; Jiang, N.; Lv, J.; Liu, L.; Zhang, L. Spatial Variations in the Response of Spring Onset of Photosynthesis of Evergreen Vegetation to Climate Factors across the Tibetan Plateau: The Roles of Interactions between Temperature, Precipitation, and Solar Radiation. *Agric. For. Meteorol.* **2023**, *335*, 109440. [[CrossRef](#)]

52. Sun, Y.; Guan, Q.; Wang, Q.; Yang, L.; Pan, N.; Ma, Y.; Luo, H. Quantitative Assessment of the Impact of Climatic Factors on Phenological Changes in the Qilian Mountains, China. *For. Ecol. Manag.* **2021**, *499*, 119594. [[CrossRef](#)]
53. Qi, Y.; Wang, H.; Ma, X.; Zhang, J.; Yang, R. Relationship between Vegetation Phenology and Snow Cover Changes during 2001–2018 in the Qilian Mountains. *Ecol. Indic.* **2021**, *133*, 108351. [[CrossRef](#)]
54. Chen, S.; Ma, M.; Wu, S.; Tang, Q.; Wen, Z. Topography Intensifies Variations in the Effect of Human Activities on Forest NPP across Altitude and Slope Gradients. *Environ. Dev.* **2023**, *45*, 100826. [[CrossRef](#)]
55. Yuan, W.; Zheng, Y.; Piao, S.; Ciais, P.; Lombardozzi, D.; Wang, Y.; Ryu, Y.; Chen, G.; Dong, W.; Hu, Z.; et al. Increased Atmospheric Vapor Pressure Deficit Reduces Global Vegetation Growth. *Sci. Adv.* **2019**, *5*, eaax1396. [[CrossRef](#)] [[PubMed](#)]
56. Deng, C.; Zhang, Y.; Wang, B.; Wang, H.; Xue, P.; Cao, Y.; Sun, L.; Cheng, S.; Cao, L.; Chen, D. Identification and Fine Mapping of *Osdsm3*, a Drought-Sensitive Gene in Rice (*Oryza sativa* L.). *Agronomy* **2023**, *13*, 2241. [[CrossRef](#)]
57. He, Y.; Yang, K.; Ren, Y.; Zou, M.; Yuan, X.; Tang, W. Causes of the Extremely Low Solar Radiation in the 2021 Growing Season over Southeastern Tibetan Plateau and Its Impact on Vegetation Growth. *Bull. Am. Meteorol. Soc.* **2023**, *104*, E359–E366. [[CrossRef](#)]
58. Li, X.; Wang, X.; Fang, Y.; Liu, D.; Huang, K.; Wang, P.; Zhang, J.; Yan, T. Phenology Advances Uniformly in Spring but Diverges in Autumn among Three Temperate Tree Species in Response to Warming. *Agric. For. Meteorol.* **2023**, *336*, 109475. [[CrossRef](#)]
59. Du, J.; Niu, J.; Gao, Z.; Chen, X.; Zhang, L.; Li, X.; Van Doorn, N.S.; Luo, Z.; Zhu, Z. Effects of Rainfall Intensity and Slope on Interception and Precipitation Partitioning by Forest Litter Layer. *CATENA* **2019**, *172*, 711–718. [[CrossRef](#)]
60. Wu, D.; Zhao, X.; Liang, S.; Zhou, T.; Huang, K.; Tang, B.; Zhao, W. Time-Lag Effects of Global Vegetation Responses to Climate Change. *Glob. Chang. Biol.* **2015**, *21*, 3520–3531. [[CrossRef](#)] [[PubMed](#)]
61. Zou, F.; Li, H.; Hu, Q. Responses of Vegetation Greening and Land Surface Temperature Variations to Global Warming on the Qinghai-Tibetan Plateau, 2001–2016. *Ecol. Indic.* **2020**, *119*, 106867. [[CrossRef](#)]
62. Zhang, Y.; Gentile, P.; Luo, X.; Lian, X.; Liu, Y.; Zhou, S.; Michalak, A.M.; Sun, W.; Fisher, J.B.; Piao, S.; et al. Increasing Sensitivity of Dryland Vegetation Greenness to Precipitation Due to Rising Atmospheric CO₂. *Nat. Commun.* **2022**, *13*, 4875. [[CrossRef](#)] [[PubMed](#)]
63. Hao, Y.; Hao, Z.; Fu, Y.; Feng, S.; Zhang, X.; Wu, X.; Hao, F. Probabilistic Assessments of the Impacts of Compound Dry and Hot Events on Global Vegetation during Growing Seasons. *Environ. Res. Lett.* **2021**, *16*, 074055. [[CrossRef](#)]
64. Wu, X.; Zhang, R.; Bento, V.A.; Leng, S.; Qi, J.; Zeng, J.; Wang, Q. The Effect of Drought on Vegetation Gross Primary Productivity under Different Vegetation Types across China from 2001 to 2020. *Remote Sens.* **2022**, *14*, 4658. [[CrossRef](#)]
65. Srivastava, A.; Yetemen, O.; Saco, P.M.; Rodriguez, J.F.; Kumari, N.; Chun, K.P. Influence of Orographic Precipitation on Coevolving Landforms and Vegetation in Semi-Arid Ecosystems. *Earth Surf. Process. Landf.* **2022**, *47*, 2846–2862. [[CrossRef](#)]
66. Zhao, W.; Duan, S.-B.; Li, A.; Yin, G. A Practical Method for Reducing Terrain Effect on Land Surface Temperature Using Random Forest Regression. *Remote Sens. Environ.* **2019**, *221*, 635–649. [[CrossRef](#)]
67. Raich, J.W.; Schlesinger, W.H. The Global Carbon Dioxide Flux in Soil Respiration and Its Relationship to Vegetation and Climate. *Tellus B* **1992**, *44*, 81–99. [[CrossRef](#)]
68. Chaparro-Suarez, I.G.; Meixner, F.X.; Kesselmeier, J. Nitrogen Dioxide (NO₂) Uptake by Vegetation Controlled by Atmospheric Concentrations and Plant Stomatal Aperture. *Atmos. Environ.* **2011**, *45*, 5742–5750. [[CrossRef](#)]
69. Ying, H.; Zhang, H.; Zhao, J.; Shan, Y.; Zhang, Z.; Guo, X.; Rihan, W.; Deng, G. Effects of Spring and Summer Extreme Climate Events on the Autumn Phenology of Different Vegetation Types of Inner Mongolia, China, from 1982 to 2015. *Ecol. Indic.* **2020**, *111*, 105974. [[CrossRef](#)]
70. Huang, F.; Liu, L.; Gao, J.; Yin, Z.; Zhang, Y.; Jiang, Y.; Zuo, L.; Fang, W. Effects of Extreme Drought Events on Vegetation Activity from the Perspectives of Meteorological and Soil Droughts in Southwestern China. *Sci. Total Environ.* **2023**, *903*, 166562. [[CrossRef](#)]
71. Wu, L.; Zhao, C.; Li, J.; Yan, Y.; Han, Q.; Li, C.; Zhu, J. Impact of Extreme Climates on Land Surface Phenology in Central Asia. *Ecol. Indic.* **2023**, *146*, 109832. [[CrossRef](#)]

Disclaimer/Publisher’s Note: The statements, opinions and data contained in all publications are solely those of the individual author(s) and contributor(s) and not of MDPI and/or the editor(s). MDPI and/or the editor(s) disclaim responsibility for any injury to people or property resulting from any ideas, methods, instructions or products referred to in the content.